

GRiD: GPU-Accelerated Rigid Body Dynamics with Analytical Gradients

Brian Plancher¹, Sabrina M. Neuman¹, Radhika Ghosal¹, Scott Kuindersma^{1,2}, Vijay Janapa Reddi¹

Abstract—We introduce GRiD: a GPU-accelerated library for computing rigid body dynamics with analytical gradients. GRiD was designed to accelerate the nonlinear trajectory optimization subproblem used in state-of-the-art robotic planning, control, and machine learning. Each iteration of nonlinear trajectory optimization requires tens to hundreds of naturally parallel computations of rigid body dynamics and their gradients. GRiD leverages URDF parsing and code generation to deliver optimized dynamics kernels that not only expose GPU-friendly computational patterns, but also take advantage of both fine-grained parallelism within each computation and coarse-grained parallelism between computations. Through this approach, when performing multiple computations of rigid body dynamics algorithms, GRiD provides as much as a 7.6x speedup over a state-of-the-art, multi-threaded CPU implementation, and maintains as much as a 2.6x speedup when accounting for I/O overhead. We release GRiD as an open-source library, so that it can be leveraged by the robotics community to easily and efficiently accelerate rigid body dynamics on the GPU.

I. INTRODUCTION

Efficient implementations of rigid body dynamics and their gradients have become key computational kernels for robotics applications. Originally required mostly for the nonlinear trajectory optimization sub-problems of model-based planning and control systems for high degrees-of-freedom robots [1], [2], [3], [4], these computational kernels are growing in importance for machine learning (ML) techniques [5], [6], [7], [8], [9].

Despite being highly accurate and optimized, existing implementations of spatial-algebra-based approaches to rigid body dynamics [10] do not take advantage of opportunities for parallelism present in the algorithm, limiting their performance [11], [12], [13], [14]. This is critical because there is natural parallelism in many bottleneck computations involving rigid body dynamics in robotics [15], [16], [9]. For example, the gradient of forward dynamics accounts for 30% to 90% of the total computational time of typical nonlinear model-predictive control (MPC) implementations [17], [18], [12], [16], and is naturally parallel across the discrete points in the trajectory.

This material is based upon work supported by the National Science Foundation (under Grant DGE1745303 and Grant 2030859 to the Computing Research Association for the CIFellows Project). Any opinions, findings, conclusions, or recommendations expressed in this material are those of the authors and do not necessarily reflect those of the funding organizations.

¹Brian Plancher, Sabrina M. Neuman, Radhika Ghosal, Scott Kuindersma, and Vijay Janapa Reddi are with the John A. Paulson School of Engineering and Applied Sciences, Harvard University, Cambridge, MA. {brian.plancher@g, rghosal@g, sneuman@seas, scotttk@seas, vj@eecs}.harvard.edu

²Scott Kuindersma is also with Boston Dynamics, Waltham, MA.

While there is a growing need for parallel computation, the performance of multi-core CPUs has been limited by thermal dissipation, enforcing a utilization wall that restricts the performance a single chip can deliver [19], [20]. This has motivated increased use of GPUs, which can provide opportunities for higher performance by supporting larger-scale parallelism within a single chip.

In this work, we introduce *GRiD*, a GPU-accelerated library for spatial-algebra-based rigid body dynamics and their analytical gradients. GRiD is designed to accelerate the nonlinear trajectory optimization subproblem used in state-of-the-art robotic planning, control, and machine learning algorithms. GRiD is optimized to use blocks of GPU threads to compute the tens to hundreds of naturally parallel computations of rigid body dynamics and their gradients found in these algorithms, and implements the more accurate spatial-algebra-based formulation of rigid body dynamics used in state-of-the-art trajectory optimization [21], [22], [23], [24].

GRiD not only unlocks the ability for nonlinear trajectory optimization to run entirely on the GPU, but when performing multiple computations of rigid body dynamics and their gradients, it also provides as much as a 7.6x speedup over a state-of-the-art, multi-threaded CPU implementation running on a high-performance workstation. GRiD also enables the use of a GPU as a rigid body physics accelerator for algorithms that are computed on a host CPU, maintaining as much as a 2.6x speedup when accounting for the I/O communication overhead between the CPU and GPU.

We release GRiD as an open-source library to enable robotics researchers to better explore and leverage the performance gains from large-scale parallelism on GPU platforms. Our library can be found at <https://github.com/robot-acceleration/grid>.

II. RELATED WORK

GRiD is designed to provide spatial-algebra-based dynamics with analytical gradients, and to accelerate them through large-scale parallelism on the GPU.

While there are many existing state-of-the-art spatial-algebra-based rigid body dynamics libraries [25], [11], [13], [26], [27], these libraries are not optimized for GPUs [16]. The exception is the recently released NVIDIA Isaac Sim [28] which supports spatial-algebra-based forward simulation, but not gradients, on the GPU.

Using automatic differentiation, differentiable physics engines can support gradient computations and have shown promise for real-time nonlinear MPC use on CPUs [29] and for accelerating machine learning, computer graphics, and

soft robotics applications [30], [31], [32], [33], [34], [35], [24], [36] on CPUs and GPUs. However, existing GPU-based differentiable physics engines are optimized for simulating thousands of interacting bodies through contact using maximal coordinate, particle, and mesh-based approaches, which are less accurate when used for rigid body robotics applications over longer time step durations [21], [24].

GPUs have also historically been used to accelerate gradient computations through numerical differentiation [37], [38]. However, these methods have been shown to have less favorable numerical properties when used for robotic planning, control, and machine learning.

As such, prior work using spatial-algebra-based approaches for planning and control on GPUs were either limited to cars, drones, and other lower degrees-of-freedom systems [15], or relied on a manually-optimized implementation of rigid body dynamics for a specific robot model [16], [39]. Finally most machine learning approaches that leverage spatial-algebra-based rigid body dynamics rely on the aforementioned physics engines [9], [28].

III. BACKGROUND

A. Computing Hardware: CPUs vs. GPUs

Compared to a multi-core CPU, a GPU is a much larger set of much simpler processors, optimized specifically for parallel computations with identical instructions (SIMD parallelism). Each GPU processor has many more arithmetic logic units (ALUs), but reduced control logic and a smaller cache memory (see Figure 1). For maximal performance, the GPU requires groups of threads within each thread block to compute the same operation on memory accessed via regular patterns. GPUs are therefore best at computing highly regular and separable computations over large working sets of data (e.g., large matrix-matrix multiplication) where much of the cache, referred to as *shared memory*, can be manually managed by the programmer. It is also worth noting that GPUs typically run at about half the clock rate of CPUs, which further hinders their performance on purely sequential code.

When leveraging a GPU as an accelerator, for each independent computation, data must be transferred from the CPU’s memory to the GPU and then back again after computations are completed. This I/O communication overhead can be amortized by performing large amounts of arithmetic operations on the GPU per each round trip memory transfer. From a design perspective, GPUs are best suited for applications which require high throughput of the compute workload, have high computational intensity, and exhibit high degrees of natural parallelism.

Our work uses NVIDIA’s CUDA [40] extensions to C++. CUDA is built around *host* (CPU) and *device* (GPU) memory and code. Special functions called *kernels* are launched from the host and then call device functions using parallel blocks of threads on the GPU. Each block’s threads access a shared cache and are guaranteed to run on the same processor, but the ordering of the blocks is not guaranteed. For more information on CUDA and its programming model we suggest reading the NVIDIA CUDA programming guide [40].

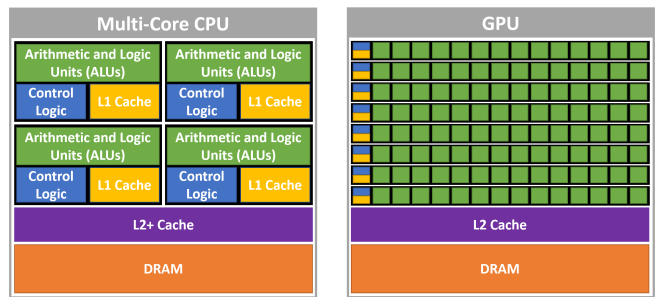


Fig. 1. High level architecture of a multi-core CPU and GPU processor.

B. Rigid Body Dynamics

State-of-the-art spatial-algebra-based rigid body dynamics algorithms [10] operate in minimal coordinates and compute functions of the the joint position $q \in \mathbb{R}^n$, velocity $\dot{q} \in \mathbb{R}^n$, acceleration $\ddot{q} \in \mathbb{R}^n$, and input torque $\tau \in \mathbb{R}^m$ that satisfy:

$$M(q)\ddot{q} + C(q, \dot{q})\dot{q} + G(q) = B(q)\tau + J(q)^T F \quad (1)$$

where $M(q) \in \mathbb{R}^{n \times n}$ is the mass matrix, $C(q, \dot{q}) \in \mathbb{R}^{n \times n}$ is a Coriolis matrix, $G(q) \in \mathbb{R}^n$ is the generalized gravity force, $B \in \mathbb{R}^{n \times m}$ maps control inputs into generalized forces, and $J(q) \in \mathbb{R}^{n \times p}$ maps any external forces or constraint forces $F \in \mathbb{R}^p$ into generalized forces. Common algorithms include: *Forward Dynamics*, computing \ddot{q} when given q, \dot{q}, τ , and optionally F ; *Inverse Dynamics*, computing τ when given q, \dot{q}, \ddot{q} and optionally F ; as well as the computations of the various terms present in Equation 1.

During computation, spatial algebra represents most quantities as operations over vectors in \mathbb{R}^6 and matrices in $\mathbb{R}^{6 \times 6}$, defined in the frame of each rigid body. These frames are numbered $i = 1$ to n such that each body’s parent λ_i is a lower number. Most rigid body dynamics algorithms operate via outward and inward loops over these frames collecting and transforming forces, accelerations, velocities, and inertias. Transformation matrices from frame λ_i to i are denoted as ${}^i X_{\lambda_i}$ and can be constructed from the rotation and translation between the two coordinate frames, which themselves are functions of the joint position q_i between those frames and constants derived from the robot’s topology. The mass distribution of each link is denoted by its spatial inertia I_i , and S_i is a joint-dependent term denoting in which directions a joint can move (and is often a constant). Finally, spatial algebra uses spatial cross product operators \times and \times^* , in which a vector is re-ordered into a matrix, and then a standard matrix multiplication is performed. This reordering is shown in Equation 2 for a vector $v \in \mathbb{R}^6$:

$$v \times = \begin{bmatrix} 0 & -v[2] & v[1] & 0 & 0 & 0 \\ v[2] & 0 & -v[0] & 0 & 0 & 0 \\ -v[1] & v[0] & 0 & 0 & 0 & 0 \\ 0 & -v[5] & v[4] & 0 & -v[2] & v[1] \\ v[5] & 0 & -v[3] & v[2] & 0 & -v[0] \\ -v[4] & v[3] & 0 & -v[1] & v[0] & 0 \end{bmatrix} \quad (2)$$

$$v \times^* = -v \times^T.$$

For more information on spatial-algebra-based rigid body dynamics we suggest reading Featherstone’s *Rigid Body Dynamics Algorithms* [10].

IV. THE GRID LIBRARY

The open-source GRiD library can be found at <https://github.com/robot-acceleration/grid>. In this section we describe its design, features and code optimization approach.

A. Code Optimization Approach

GRiD builds on recent work which designed a manually-optimized GPU implementation of rigid body dynamics gradients for a single robot model, a seven-link serial chain manipulator [39]. In this section we detail the generalizations, and subsequent optimizations, that enable GRiD to accelerate both a much larger class of robot models and additional rigid body dynamics algorithms.

Previous work has shown that a robot’s topology and joint types define many structured sparsity patterns and opportunities for both coarse and fine-grained parallelism in the resulting spatial-algebra-based rigid body dynamics algorithms [41], [11], [13], [39], [42]. We take advantage of this parallelism through multi-threading both within and between each computation of each algorithm. For example, within each independent gradient computation, each column of that computation can be computed independently, and within those computations each entry in each matrix-matrix or matrix-vector multiplication can be computed independently. GRiD is able to achieve high performance by taking advantage of this large-scale parallelism by using a block of threads on a GPU for each computation of each algorithm.

However, in order for the GPU to effectively take advantage of this parallelism, the target algorithm needs to be refactored to remove synchronization points and coalesce both memory accesses as well as computational operations. We adapt the refactoring in previous work [39] and generalize it from only targeting a seven-link serial chain manipulator to target robots with any branched kinematic tree topology (see example in Figure 2). To do this we need to inject additional optimizations to account for the possibility of multiple branching points at different levels of the tree.

We note that since dependencies during rigid body dynamics algorithms are between parent and child frames, we can, in parallel, compute each level of the kinematic tree in a breadth-first search manner during serial loops of the underlying algorithms. For example, the RNEA algorithm (shown in Algorithm 1) computes the temporary variables v, a as a function of the parent v, a in the first loop (on lines 4 and 5) and then computes the temporary variable f as a function of its child f in the second loop (on line 9). This parent-child dependency implies that for the rigid body robot shown in Figure 2 we can compute the loops serially over levels of the tree with each level in parallel. That is, we can compute in parallel the values associated with frame 0, followed by frames 1, and 5, followed by frames 2, 4, and 6, followed by frame 3 during the first loop, and in the

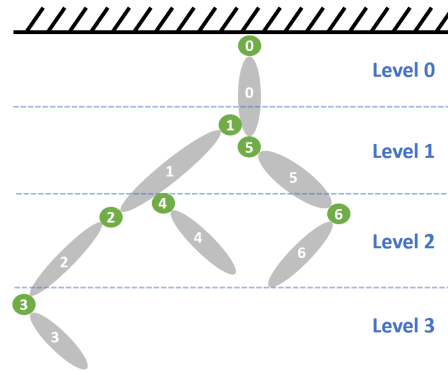


Fig. 2. An example robot topology.

Algorithm 1 RNEA(q, \dot{q}, \ddot{q}, F) $\rightarrow c$

- 1: $v_0 = 0, a_0 = \text{gravity}$
 - 2: **for** link $i = 1 : n$ **do**
 - 3: Compute ${}^i X_{\lambda_i}(q), S_i(q), I_i, f^{\text{ext}}(q, F)$
 - 4: $v_i = {}^i X_{\lambda_i} v_{\lambda_i} + S_i \dot{q}_i$
 - 5: $a_i = {}^i X_{\lambda_i} a_{\lambda_i} + S_i \ddot{q}_i + v_i \times S_i \dot{q}_i$
 - 6: $f_i = I_i a_i + v_i \times^* I_i v_i - f^{\text{ext}}$
 - 7: **for** link $i = n : 1$ **do**
 - 8: $c_i = S_i^T f_i$
 - 9: $f_{\lambda_i} += {}^i X_{\lambda_i}^T f_i$
-

opposite order during the second loop. GRiD also performs loop unrolling on these remaining serial loops to enable the compiler to easily optimize the resulting code.

Since out-of-order computations and irregular data access patterns are also inefficient to compute on a GPU, it is important to avoid these, even at the expense of creating large numbers of temporary variables. This is particularly important when working with the spatial cross product operations (Equation 2) as they result in a re-ordering and expansion of the dimension of the input vector.

However, when supporting arbitrarily large robots it is import to also ensure that the temporary variables fit into the GPU cache. We therefore generate many temporary variables and determine at code generation time if, due to memory constraints, it is necessary to avoid several of the temporary memory computations in order to support robots with many degrees-of-freedom (dof). For example, the code generated for the Atlas humanoid, with over 30 dof, does not compute each $v \times$ matrix in parallel and then use standard threaded matrix multiplication, as suggested in previous work [39]. Instead the code performs the sparse $v_1 \times v_2$ operation in a few parallel threads, trading off a slight latency penalty for a large savings in shared memory usage.

GRiD also leverages the robot’s topology to determine sparsity patterns in the many temporary variables needed for the gradient computations. As such, columns of temporary memory variables that would be all zeros are skipped and shared memory is compressed to effectively remove those

columns. While this does complicate the memory addressing schema, the required offsets are computed and cached at code generation time, minimizing the impact on latency. For most robot models this leads to significant savings. For example, this approach reduces the shared memory required for the the quadruped robot HyQ [43] by more than 60%.

Wherever pointer offsets and other control flow switches cannot be determined at compile time, GRiD employs, non-branching *if/else* constructs (e.g., `result = flag*val1 + !flag*val2`) to avoid the branching performance penalty.

Finally, GRiD employs further optimizations for certain classes of robot models. For example, for all single chain robots, the parent’s frame number is always one less than the child’s. For these robots, the code generated by GRiD will remove any indirect references to the parent (or child) frame number and instead simply subtract (or add) one.

B. Current Features

The GRiD library currently fully supports any robot model consisting of revolute, prismatic, and fixed joints and implements the following rigid body dynamics algorithms: the Recursive Newton Euler Algorithm (RNEA) for inverse dynamics [10]; the direct inverse of mass matrix (M^{-1}) [12]; forward dynamics via the $-M^{-1} * (\tau - \text{RNEA}(q, \dot{q}, 0))$ approach; the analytical gradient of inverse dynamics [12]; and also the analytical gradient of forward dynamics via the $\frac{\partial \dot{q}}{\partial u} = -M^{-1} \frac{\partial \text{RNEA}(q, \dot{q}, \ddot{q})}{\partial u}$ approach [12]. Future work presently in development will extend this core foundation with additional algorithms and joint types (see Section VI).

C. Design

Our overarching design methodology was to make GRiD easily adoptable and extensible by other robotics researchers. As such, the resulting optimized CUDA C++ code is designed to be header-only with only a single dependency, the standard `cuda_runtime.h` library.¹

The GRiD library is also designed to be used by both GPU experts and novices. As such, we provide an API that allows users to integrate GRiD either directly into their existing CUDA code or through standard CPU C++ function calls.

We also provide functions to automatically initialize and allocate all necessary memory on the CPU and GPU.

Finally, the GRiD library is built using a set of modular open-source packages (shown in Figure 3) to enable easy extension, and re-use by other robotics researchers. Our **GRiD** package wraps and automates our GPU code generation engine (**GRiDCodeGenerator**), a self-contained URDF parser (**URDFParser**), and a set of reference implementations of rigid body dynamics algorithms (**RBDReference**) that can be used for code validation and testing.

We also provide the benchmark experiments as described in Section V as a separate package (**GRiDBenchmarks**), as they require the support of additional external libraries.

¹Even during URDF parsing and code generation, GRiD only requires the `beautifulsoup4`, `lxml`, `numpy`, and `sympy` Python libraries.

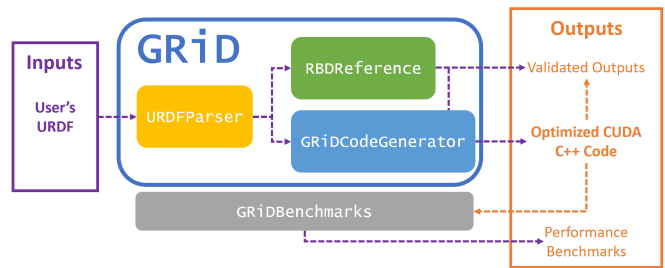


Fig. 3. The GRiD library package ecosystem, showing how a user’s URDF file can be transformed into optimized CUDA C++ code which can then be validated against reference outputs and benchmarked for performance.

V. PERFORMANCE BENCHMARKS

We benchmark the GRiD library against the Pinocchio library [13],² a state-of-the-art CPU-implementation of rigid body dynamics that supports optimized CPU code generation of both rigid body dynamics and its analytical gradients. Source code accompanying this evaluation can be found at <https://github.com/robot-acceleration/GRiDBenchmarks>.

A. Methodology

All results were collected on a high-performance workstation with a 3.8GHz eight-core Intel Core i7-10700K CPU and a 1.44GHz NVIDIA GeForce GTX 3080 GPU running Ubuntu 20.04 and CUDA 11.4. For clean timing measurements on the CPU, we disabled TurboBoost and fixed the clock frequency to the maximum. Code was compiled with `Clang 12` and `g++9.4`, and time was measured with the Linux system call `clock_gettime()`, using `CLOCK_MONOTONIC` as the source.

We compare timing results across three robot models: the 7 degrees-of-freedom (dof) Kuka LBR IIWA-14 manipulator [44], the 12 dof HyQ quadruped [43], and the 30 dof Atlas humanoid [45], [46]. For single computation and multiple computation latency, we took the average of one million, and one hundred thousand trials, respectively.

B. Multiple Computation Latency

To characterize our performance in a typical nonlinear trajectory optimization scenario which use tens to hundreds of naturally parallel computations of dynamics algorithms, we evaluate the latency for $N = 16, 32, 64, 128,$ and 256 computations of the gradient of forward dynamics using Pinocchio and GRiD across robot models in Figure 4. These times are broken down into computation time on the CPU or GPU and the GPU I/O overhead. The plot is overlaid with the speedup (or slowdown) of GRiD as compared to Pinocchio both in terms of pure computation and including I/O overhead. We use the gradient of forward dynamics as our representative kernel as it uses many of the other kernels as sub-routines, and is the most computationally intense kernel, clearly demonstrating scaling trends.

²We used the `pinocchio3-preview` branch to ensure we were using the latest, most optimized, code.

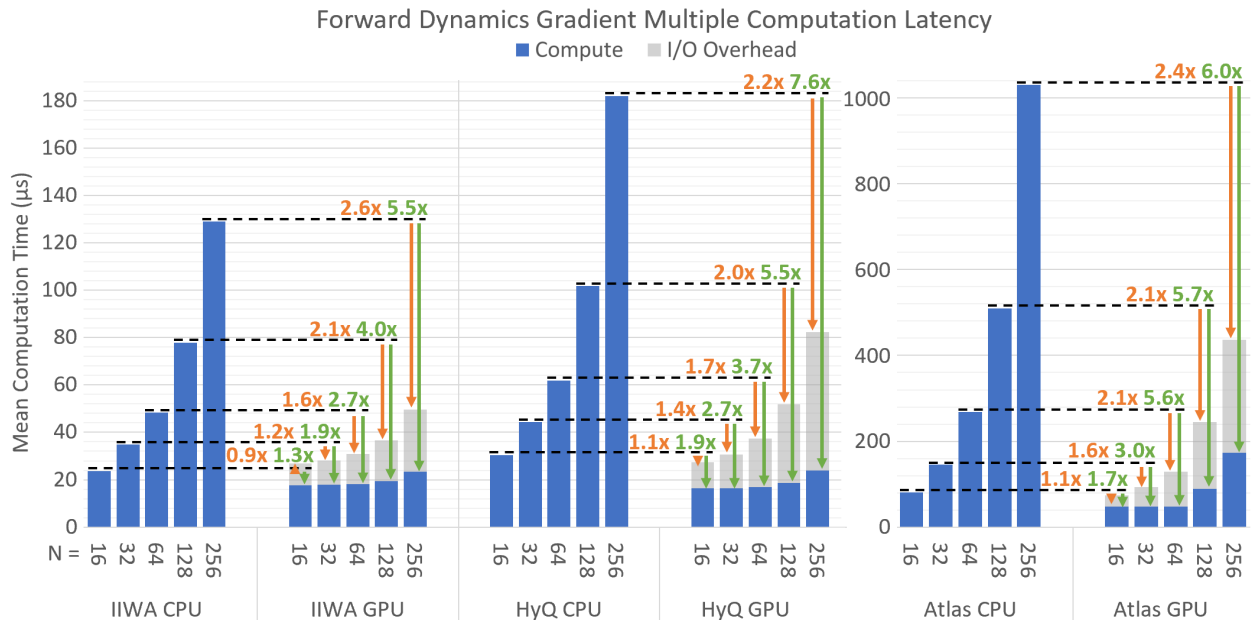


Fig. 4. Latency (including GPU I/O overhead) for $N = 16, 32, 64, 128,$ and 256 computations of the gradient of forward dynamics for both the Pinocchio CPU baseline and the GRiD GPU library for various robot models (IIWA, HyQ, and Atlas as described in Section V-A). Overlaid is the speedup (or slowdown) of GRiD as compared to Pinocchio both in terms of pure computation and including I/O overhead.

The GPU outperforms the CPU on all but one of the multiple computation latency tests, even when accounting for I/O. In the one test where the CPU is faster—for the fewest computations, including I/O, for IIWA, the smallest robot with only a single limb—the GPU is still 0.9x as fast.

Even on the CPU, this benchmark shows how important it is to take advantage of coarse-grained parallelism between computations. For example, the gradient of forward dynamics kernel (∇FD in Table I) took 2.5, 3.8, and 22.7 μs for a single computation for IIWA, HyQ, and Atlas respectively. If we ran it 256 times serially it would therefore take over 648, 983, and 5806 μs . As Figure 4 shows, computing it in parallel on 8-cores only takes 129, 182, 1031 μs , saving 80-82% of the computation time.

However, since the CPU only has 8 cores, it is unable to efficiently scale to take advantage of high numbers of naturally parallel computations, taking 5.4x, 6.0x, and 12.8x as long to compute $N = 256$ as compared to $N = 16$ for IIWA, HyQ, and Atlas respectively.

The GPU, on the other hand, is designed to scale to higher numbers of computations without incurring a latency penalty by launching independent blocks of threads for each computation. In fact, for IIWA and HyQ, $N = 256$ takes only 1.3x and 1.5x as long as $N = 16$. This leads to the GPU outperforming the CPU by 5.5x and 7.6x for $N = 256$, and maintaining a 2.6x and 2.2x speedup when including I/O.

For the much higher-dof Atlas robot, the GPU still outperforms the CPU for $N = 256$ by 6.0x, and 2.4x when including I/O. However, unlike with IIWA and HyQ, this performance increase is very similar to the increase at $N = 128$. This stall in performance improvement is caused by the large amount of shared memory needed for Atlas’s 30 dof which starts to

TABLE I
SINGLE COMPUTATION LATENCY IN μs PER ALGORITHM AND ROBOT (ID = INVERSE DYNAMICS, MINV = DIRECT MINV, FD = FORWARD DYNAMICS AND ∇ INDICATES THE GRADIENT OF THAT ALGORITHM)

Algorithm	CPU			GPU		
	IIWA	HyQ	Atlas	IIWA	HyQ	Atlas
ID	0.2	0.3	1.1	3.0	3.2	8.0
Minv	0.5	0.7	3.2	5.2	5.6	17.4
FD	0.9	1.2	5.3	7.7	6.9	22.4
∇ ID	1.4	2.1	10.0	6.3	5.8	19.5
∇ FD	2.5	3.8	22.7	12.9	11.0	42.1

limit the number of parallel blocks of threads that can fit concurrently on the GPU hardware.

Finally, we note that, for the GPU, I/O overhead accounts for 53-71% of the total time for $N = 256$. This is why, in general, the GPU is best used when either the entire algorithm can reside on the GPU, or the computation done on to the GPU is quite large and time consuming.

C. Single Computation Latency Scaling

For further analysis of the GPU performance benefits demonstrated in Section V-B, we plot the latency scaling, excluding I/O overheads, of a single computation of each rigid body dynamics algorithm, from IIWA to HyQ and IIWA to Atlas, on both the CPU and GPU in Figure 5, and list absolute timings in Table I. We also plot the scaling of the robots’ dof as a measure of their increased complexity.

We find that the GPU is able to scale to more complex robots and algorithms better than the CPU by taking advantage of fine-grained parallelism induced by independent robot

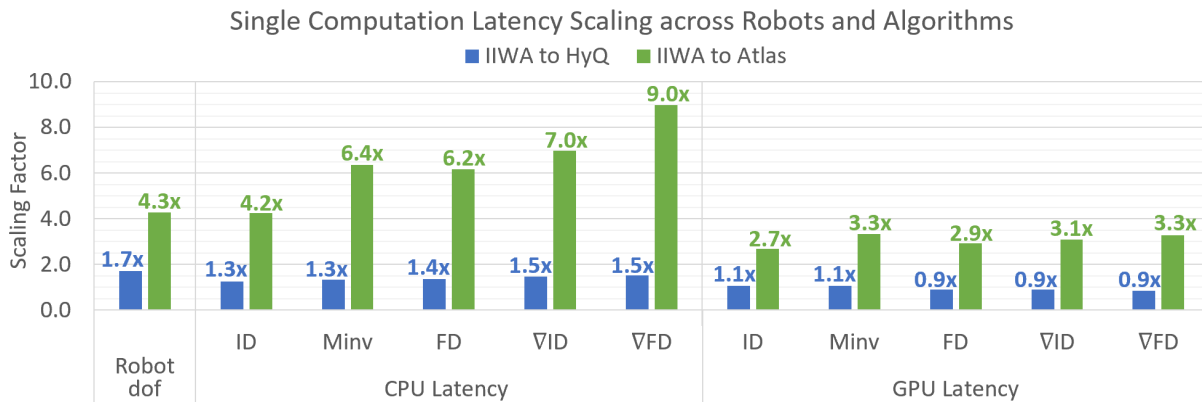


Fig. 5. The scaling of single computation latency from IIWA to HyQ and IIWA to Atlas for both the Pinocchio CPU baseline and the GRiD GPU library for various rigid body dynamics algorithms (ID = Inverse Dynamics, Minv = Direct Minv, FD = Forward Dynamics and ∇ indicates the gradient of that algorithm). We also plot the scaling of the robots’ dof as a measure of their increased complexity.

limbs and the independent columns of gradient computations. This is why GPUs are most advantageous when used on computations where they can take advantage of both fine and coarse-grained parallelism. As expected (and consistent with previous work [39]), the GPU is slower on a single computation than the CPU, but the GPU demonstrates better scalability across both algorithm and robot complexity. For example, for ∇ FD, the GPU and CPU take $12.9\mu\text{s}$ versus $2.5\mu\text{s}$ for IIWA—a difference of 5.1x—but for the more complex Atlas, they take only $42.1\mu\text{s}$ versus $22.7\mu\text{s}$ —a significantly reduced difference of 1.9x (Table I).

On the CPU, the latency of each algorithm scales directly with its computational intensity, with the gradients requiring significantly more computation (see Table I). The most computationally intensive algorithm, the forward dynamics gradient (∇ FD), takes 2.5, 3.8, and $22.7\mu\text{s}$ for IIWA, HyQ, and Atlas, while the simplest algorithm, inverse dynamics (ID) takes 0.2, 0.3, and $1.1\mu\text{s}$ —a 10.2x to 21.5x slowdown.

CPU latency also scales with the dof of the robot (Figure 5). For example, as the robot’s dof increases by a factor of 1.7x from IIWA to HyQ, the computation time also increase by 1.3x, for the $O(N)$ ID algorithm, up to 1.5x, for the $O(N^2)$ ∇ FD algorithm. It appears that this strong performance is due to the code generation taking advantage of the sparsity induced by HyQ’s independent limbs and the many shared computations in the gradient computations. However, these optimizations are mitigated by the Atlas model, which is more complex with a multi-link torso and a much larger 30 dof. Atlas has 4.3x the dof of IIWA, but has a 4.2x (ID) to 9.0x (∇ FD) slowdown on the CPU.

By contrast, the GPU is able improve its scalability by not only taking advantage of sparsity and shared computations, but *also the opportunities for fine-grained parallelism* caused by both independent limbs in complex robot models, and independent columns of the gradient computations. For example, Table I shows that by taking advantage of parallelism in the gradient computations, the GPU only takes 12.9, 11.0, and $42.1\mu\text{s}$ (for IIWA, HyQ, Atlas) to compute the most computationally-intensive algorithm, the gradient of forward

dynamics (∇ FD), as compared to 3.0, 3.2, and $8.0\mu\text{s}$ for the simplest algorithm, inverse dynamics (ID)—a slowdown of only 3.4x to 5.3x, and a significant reduction from the CPU’s 10.2x to 21.5x slowdown for these algorithms. Similarly, Figure 5 shows that by leveraging limb-based parallelism, the GPU computes forward dynamics (FD) and both gradients (∇ ID, ∇ FD) faster for HyQ than for IIWA, and only has a 2.7x to 3.3x slowdown from IIWA to Atlas, again a significant reduction from the CPU’s 4.2x to 9.0x.

VI. CONCLUSION AND FUTURE WORK

In this work, we introduce GRiD, a GPU-accelerated rigid body dynamics library with analytical gradients. We found that by leveraging large-scale parallelism when performing multiple computations of rigid body dynamics algorithms, GRiD can provide as much as a 7.6x speedup over a state-of-the-art, multi-threaded CPU implementation and maintains as much as a 2.6x speedup when including I/O overhead.

There are many promising directions for future work to extend the functionality and versatility of the GRiD library. We have current work under development to expand GRiD to support the full breadth of rigid body dynamics algorithms and robot models supported by current state-of-the-art CPU spatial-algebra-based rigid body dynamics libraries [25], [11], [13], [26], [27]. Additionally, we are developing wrappers to our C++ host functions in higher level languages to make it even easier to leverage GRiD.

We would like to explore emerging rigid body dynamics algorithms and alternate formulations and implementations of rigid body dynamics, which may expose additional parallelism and improve overall performance [47], [48], [49], [50], [51], [52], [53]. We would also like to add support for contact and integrate these accelerated dynamics implementations into existing robotics software frameworks [54], [55], [56], [16], [57]. This would increase both GRiD’s ease-of-use and applicability to more robotics researchers. Finally, building out increased support for more trajectory optimization, MPC, and ML algorithms running entirely on the GPU would further increase the performance benefits from integrating GRiD into these approaches.

REFERENCES

- [1] F. Farshidian, E. Jelavic, A. Satapathy, M. Gifftthaler, and J. Buchli, "Real-time motion planning of legged robots: A model predictive control approach," in *2017 IEEE-RAS 17th International Conference on Humanoid Robotics*.
- [2] M. Gifftthaler, M. Neunert, M. Stäuble, J. Buchli, and M. Diehl, "A Family of Iterative Gauss-Newton Shooting Methods for Nonlinear Optimal Control." [Online]. Available: <http://arxiv.org/abs/1711.11006>
- [3] B. Plancher and S. Kuindersma, "Realtime model predictive control using parallel ddp on a gpu," in *Toward Online Optimal Control of Dynamic Robots Workshop at the 2019 International Conference on Robotics and Automation (ICRA)*, Montreal, Canada, May, 2019.
- [4] S. Kleff, A. Meduri, R. Budhiraja, N. Mansard, and L. Righetti, "High-frequency nonlinear model predictive control of a manipulator," *Preprint*, 2020.
- [5] J. Carius, F. Farshidian, and M. Hutter, "Mpc-net: A first principles guided policy search," *IEEE Robotics and Automation Letters*, vol. 5, no. 2, p. 2897–2904, Apr 2020. [Online]. Available: <http://dx.doi.org/10.1109/LRA.2020.2974653>
- [6] M. Omer, R. Ahmed, B. Rosman, and S. F. Babikir, "Model predictive-actor critic reinforcement learning for dexterous manipulation," in *2020 International Conference on Computer, Control, Electrical, and Electronics Engineering (ICCCEEE)*, 2021, pp. 1–6.
- [7] D. Hoeller, F. Farshidian, and M. Hutter, "Deep value model predictive control," in *Proceedings of the Conference on Robot Learning*, ser. Proceedings of Machine Learning Research, L. P. Kaelbling, D. Kragic, and K. Sugiura, Eds., vol. 100, 30 Oct–01 Nov 2020, pp. 990–1004. [Online]. Available: <http://proceedings.mlr.press/v100/hoeller20a.html>
- [8] S. Gros and M. Zanon, "Reinforcement learning for mixed-integer problems based on mpc," 2020.
- [9] A. S. Morgan, D. Nandha, G. Chalvatzaki, C. D'Eramo, A. M. Dollar, and J. Peters, "Model predictive actor-critic: Accelerating robot skill acquisition with deep reinforcement learning," 2021.
- [10] R. Featherstone, *Rigid Body Dynamics Algorithms*. Springer.
- [11] M. Frigerio, J. Buchli, D. G. Caldwell, and C. Semini, "RobCoGen: A code generator for efficient kinematics and dynamics of articulated robots, based on Domain Specific Languages," vol. 7, no. 1, pp. 36–54.
- [12] J. Carpentier and N. Mansard, "Analytical derivatives of rigid body dynamics algorithms," in *Robotics: Science and Systems*, 2018.
- [13] J. Carpentier, G. Saurel, G. Buondonno, J. Mirabel, F. Lamiroux, O. Stasse, and N. Mansard, "The pinocchio c++ library : A fast and flexible implementation of rigid body dynamics algorithms and their analytical derivatives," in *2019 IEEE/SICE International Symposium on System Integration (SII)*, 2019, pp. 614–619.
- [14] S. Neuman, T. Koolen, J. Drean, J. Miller, and S. Devadas, "Benchmarking and workload analysis of robot dynamics algorithms," in *2019 IEEE/RSJ International Conference on Intelligent Robots and Systems (IROS)*, 2019.
- [15] G. Williams, A. Aldrich, and E. A. Theodorou, "Model predictive path integral control: From theory to parallel computation," *Journal of Guidance, Control, and Dynamics*, vol. 40, no. 2, pp. 344–357, 2017.
- [16] B. Plancher and S. Kuindersma, "A Performance Analysis of Parallel Differential Dynamic Programming on a GPU," in *International Workshop on the Algorithmic Foundations of Robotics (WAFR)*.
- [17] J. Koenemann, A. Del Prete, Y. Tassa, E. Todorov, O. Stasse, M. Bennewitz, and N. Mansard, "Whole-body Model-Predictive Control applied to the HRP-2 Humanoid," in *Proceedings of the IEEE/RSJ International Conference on Intelligent Robots*.
- [18] M. Neunert, C. de Crousaz, F. Furrer, M. Kamel, F. Farshidian, R. Siegwart, and J. Buchli, "Fast nonlinear Model Predictive Control for unified trajectory optimization and tracking," in *2016 IEEE International Conference on Robotics and Automation (ICRA)*, pp. 1398–1404.
- [19] H. Esmaeilzadeh, E. Blem, R. St. Amant, K. Sankaralingam, and D. Burger, "Dark Silicon and the End of Multicore Scaling," in *Proceedings of the 38th Annual International Symposium on Computer Architecture*, ser. ISCA '11. ACM, pp. 365–376.
- [20] G. Venkatesh, J. Sampson, N. Goulding, S. Garcia, V. Bryksin, J. Lugo-Martinez, S. Swanson, and M. B. Taylor, "Conservation Cores: Reducing the Energy of Mature Computations," in *Proceedings of the Fifteenth Edition of ASPLOS on Architectural Support for Programming Languages and Operating Systems*, ser. ASPLOS XV. ACM, pp. 205–218.
- [21] T. Erez, Y. Tassa, and E. Todorov, "Simulation tools for model-based robotics: Comparison of bullet, havok, mujoco, ode and physx," in *2015 IEEE international conference on robotics and automation (ICRA)*. IEEE, 2015, pp. 4397–4404.
- [22] J.-P. Sleiman, F. Farshidian, M. V. Minniti, and M. Hutter, "A unified mpc framework for whole-body dynamic locomotion and manipulation," *IEEE Robotics and Automation Letters*, vol. 6, no. 3, pp. 4688–4695, 2021.
- [23] L. Drnack and Y. Zhao, "Robust trajectory optimization over uncertain terrain with stochastic complementarity," *IEEE Robotics and Automation Letters*, vol. 6, no. 2, pp. 1168–1175, 2021.
- [24] C. D. Freeman, E. Frey, A. Raichuk, S. Girgin, I. Mordatch, and O. Bachem, "Brax – a differentiable physics engine for large scale rigid body simulation," 2021.
- [25] E. Todorov, T. Erez, Y. Tassa, and tassa, "MuJoCo: A physics engine for model-based control," in *Proceedings of the IEEE/RSJ International Conference on Intelligent Robots*.
- [26] T. Koolen and R. Deits, "Julia for robotics: simulation and real-time control in a high-level programming language," in *2019 International Conference on Robotics and Automation (ICRA)*, 2019, pp. 604–611.
- [27] K. Werling, D. Omens, J. Lee, I. Exarchos, and C. K. Liu, "Fast and feature-complete differentiable physics for articulated rigid bodies with contact," *arXiv preprint arXiv:2103.16021*, 2021.
- [28] V. Makovychuk, L. Wawrzyniak, Y. Guo, M. Lu, K. Storey, M. Macklin, D. Hoeller, N. Rudin, A. Allshire, A. Handa, and G. State, "Isaac gym: High performance gpu-based physics simulation for robot learning," 2021.
- [29] M. Neunert, M. Gifftthaler, M. Frigerio, C. Semini, and J. Buchli, "Fast Derivatives of Rigid Body Dynamics for Control, Optimization and Estimation," in *IEEE International Conference on Simulation, Modeling, and Programming for Autonomous Robots (SIMPAN)*.
- [30] J. Bender, M. Müller, and M. Macklin, "A survey on position based dynamics, 2017," in *Proceedings of the European Association for Computer Graphics: Tutorials*, 2017, pp. 1–31.
- [31] F. de Avila Belbute-Peres, K. Smith, K. Allen, J. Tenenbaum, and J. Z. Kolter, "End-to-end differentiable physics for learning and control," in *Advances in neural information processing systems*, 2018, pp. 7178–7189.
- [32] J. Degraeve, M. Hermans, J. Dambre, *et al.*, "A differentiable physics engine for deep learning in robotics," *Frontiers in neurobotics*, vol. 13, p. 6, 2019.
- [33] Y. Hu, J. Liu, A. Spielberg, J. B. Tenenbaum, W. T. Freeman, J. Wu, D. Rus, and W. Matusik, "Chainqueen: A real-time differentiable physical simulator for soft robotics," in *2019 International Conference on Robotics and Automation (ICRA)*. IEEE, 2019, pp. 6265–6271.
- [34] J. Austin, R. Corrales-Fatou, S. Wytznner, and H. Lipson, "Titan: A parallel asynchronous library for multi-agent and soft-body robotics using nvidia cuda," in *2020 IEEE International Conference on Robotics and Automation (ICRA)*. IEEE, 2020, pp. 7754–7760.
- [35] Y. Hu, L. Anderson, T.-M. Li, Q. Sun, N. Carr, J. Ragan-Kelley, and F. Durand, "DiffTaichi: Differentiable programming for physical simulation," in *International Conference on Learning Representations (ICLR)*, 2020.
- [36] E. Heiden, M. Macklin, Y. S. Narang, D. Fox, A. Garg, and F. Ramos, "DiSECT: A Differentiable Simulation Engine for Autonomous Robotic Cutting," in *Proceedings of Robotics: Science and Systems*, Virtual, July 2021.
- [37] P. Micikevicius, "3d finite difference computation on gpus using cuda," in *Proceedings of 2nd workshop on general purpose processing on graphics processing units*, 2009, pp. 79–84.
- [38] D. Michéa and D. Komatitsch, "Accelerating a three-dimensional finite-difference wave propagation code using gpu graphics cards," *Geophysical Journal International*, vol. 182, no. 1, pp. 389–402, 2010.
- [39] B. Plancher, S. M. Neuman, T. Bourgeat, S. Kuindersma, S. Devadas, and V. J. Reddi, "Accelerating robot dynamics gradients on a cpu, gpu, and fpga," *IEEE Robotics and Automation Letters*, vol. 6, no. 2, pp. 2335–2342, 2021.
- [40] NVIDIA, *NVIDIA CUDA C Programming Guide*, version 9.1 ed. [Online]. Available: http://docs.nvidia.com/cuda/pdf/CUDA_C-Programming_Guide.pdf
- [41] R. Featherstone, "Exploiting sparsity in operational-space dynamics," *The International Journal of Robotics Research*, vol. 29, no. 10, pp. 1353–1368, 2010. [Online]. Available: <https://doi.org/10.1177/0278364909357644>

- [42] S. M. Neuman, B. Plancher, T. Bourgeat, T. Tambe, S. Devadas, and V. J. Reddi, "Robomorphic computing: A design methodology for domain-specific accelerators parameterized by robot morphology," ser. ASPLOS 2021. New York, NY, USA: Association for Computing Machinery, 2021, p. 674–686. [Online]. Available: <https://doi-org.ezp-prod1.hul.harvard.edu/10.1145/3445814.3446746>
- [43] C. Semini, N. G. Tsagarakis, E. Guglielmino, M. Focchi, F. Cannella, and D. G. Caldwell, "Design of hyq - a hydraulically and electrically actuated quadruped robot," *IMEchE Part I: Journal of Systems and Control Engineering*, vol. 225, no. 6, pp. 831–849, 2011.
- [44] KUKA AG, "Lbr iiwa — kuka ag," Accessed in 2020, available: [kuka.com/products/robotics-systems/industrial-robots/lbr-iiwa](https://www.kuka.com/products/robotics-systems/industrial-robots/lbr-iiwa). [Online]. Available: <https://www.kuka.com/products/robotics-systems/industrial-robots/lbr-iiwa>
- [45] Boston Dynamics, "Atlas," Accessed in 2021, available: <https://www.bostondynamics.com/atlas>. [Online]. Available: <https://www.bostondynamics.com/atlas>
- [46] S. Kuindersma, R. Deits, M. Fallon, A. Valenzuela, H. Dai, F. Permenter, T. Koolen, P. Marion, and R. Tedrake, "Optimization-based locomotion planning, estimation, and control design for Atlas," vol. 40, no. 3, pp. 429–455.
- [47] R. Featherstone, "A divide-and-conquer articulated-body algorithm for parallel $O(\log(n))$ calculation of rigid-body dynamics. part 1: Basic algorithm," *The International Journal of Robotics Research*, vol. 18, no. 9, pp. 867–875, 1999.
- [48] K. Yamane and Y. Nakamura, "Comparative Study on Serial and Parallel Forward Dynamics Algorithms for Kinematic Chains," vol. 28, no. 5, pp. 622–629.
- [49] Y. Yang, Y. Wu, and J. Pan, "Parallel Dynamics Computation Using Prefix Sum Operations," vol. 2, no. 3, pp. 1296–1303.
- [50] J. Brüdigam and Z. Manchester, "Linear-time variational integrators in maximal coordinates," 2020.
- [51] J. Nganga and P. M. Wensing, "Accelerating second-order differential dynamic programming for rigid-body systems," *IEEE Robotics and Automation Letters*, pp. 1–1, 2021.
- [52] S. Singh, R. P. Russell, and P. M. Wensing, "Efficient analytical derivatives of rigid-body dynamics using spatial vector algebra," 2021.
- [53] S. Echeandia and P. M. Wensing, "Numerical methods to compute the coriolis matrix and christoffel symbols for rigid-body systems," *Journal of Computational and Nonlinear Dynamics*, vol. 16, no. 9, 07 2021, 091004. [Online]. Available: <https://doi.org/10.1115/1.4051169>
- [54] R. Tedrake and the Drake Development Team, "Drake: A planning, control, and analysis toolbox for nonlinear dynamical systems." [Online]. Available: <http://drake.mit.edu>
- [55] G. Brockman, V. Cheung, L. Pettersson, J. Schneider, J. Schulman, J. Tang, and W. Zaremba, "Openai gym," 2016.
- [56] M. Gifithaler, M. Neunert, M. Stäuble, and J. Buchli, "The control toolbox — an open-source c++ library for robotics, optimal and model predictive control," *2018 IEEE International Conference on Simulation, Modeling, and Programming for Autonomous Robots (SIMPAN)*, pp. 123–129, 2018.
- [57] T. Howell, B. Jackson, and Z. Manchester, "Altro: A fast solver for constrained trajectory optimization," in *Proceedings of (IROS) IEEE/RSJ International Conference on Intelligent Robots and Systems*, November 2019, pp. 7674 – 7679.